

# Phonon laser in cavity magnomechanics

Ming-Song Ding<sup>a</sup>, Li Zheng<sup>b</sup>, Chong Li<sup>a,\*</sup>

<sup>a</sup>*School of Physics, Dalian University of Technology, Dalian 116024, China*

<sup>b</sup>*Information Science and Engineering College, Dalian Polytechnic University, Dalian 116034, China*

## Abstract

The phonon analog of an optical laser has become the focus of research. We theoretically study phonon lasing in a cavity magnomechanical system, which consist of a microwave cavity, a YIG sphere and the uniform external bias magnetic field. This system can realize the phonon-magnon coupling and the cavity photon-magnon coupling via magnetostrictive interaction and magnetic dipole interaction respectively, the magnons are driven directly by a strong microwave field simultaneously. We find that the phonon laser can be well controlled by an adjustable external magnetic field without changing other parameters, which provides an additional degree of freedom compared to the phonon laser in optomechanical systems. Moreover, with the experimentally feasible parameters, threshold power in our system is close to the threshold power of phonon laser in optomechanical systems. Our results provide a theoretical basis for the realization of phonon lasers in magnomechanical systems.

## 1. Introduction

In recent years, cavity magnomechanical system has been becoming a novel platforms for realizing quantum coherence and coupling between magnons, cavity photons and phonons. Among them, the coupling between photons and magnons is realized by the magnetic dipole interaction. The interaction between magnons and phonons is based on the magnetostrictive force. As we know the traditional optomechanical systems use radiation force [1, 2, 4, 3, 5, 6, 7, 8, 9, 10, 11, 12, 13, 14], electrostatic force [15, 16], and piezoelectric force [17] for coupling phonon with optical or microwave photons, but they all intrinsically lack good tunability. The emergence of magnetostrictive force provides us with a new way to achieve different information carriers [18, 19]. Because the magnons are collective excitation of magnetization, whose frequency can be easily adjusted by external bias magnetic field, the magnetostrictive force plays a major role in magnetic materials. It is important to choose an excellent magnetic material. The emergence of magnetic insulator yttrium iron garnet (YIG) provides important help for the realization of the coupling between magnons and phonons. The YIG sphere is introduced into the cavity magnomechanical system as an effective mechanical resonator. The varying magnetization caused by the excitation of the magneton in the YIG sphere results in the geometric deformation of the surface, introducing the coupling between magnon and phonon modes. YIG has rich magnonic nonlinearities and the characteristic of low loss in different information carriers, these excellent properties make it possible to find many interesting and important phenomena in cavity magnomechanical systems and other quantum systems. And it provides a good opportunity for realizing a highly tunable quantum system for the informa-

tion processing. Based on it, a lot of theoretical and experimental researches have been done. J. Q. You *et al.* have found the bistability of cavity magnon polaritons [20], G. S. Agarwal *et al.* have reported that the tripartite entanglement among magnons, cavity photons, and phonons can be achieved by optimal parameters [18]. Furthermore, high-order sideband generation [22, 23], magnon Kerr effect [21], the light transmission in cavity-magnon system [24] and other researches were also studied [25, 26, 27, 28, 29, 30].

Phonon laser as a novel laser has been developed rapidly, it generates coherent sound oscillations (mechanical vibration) by optical pumping. Just like traditional optical laser [31, 32], phonon laser can be considered as an analogue of a two-level optical laser which is provided by phonon mediated transitions between two optical supermodes [33, 34, 35]. These supermodes correspond to the ground and excited states respectively, and the mechanical mode (phonons) mediates the transition between them. As early as 2003, Chen, J. and Khurgin have verified the feasibility of phonon lasers and proposed a scheme to realize phonon lasers [36]. Then single trapped ions and quantum dots have been utilized in the fields of phonon laser [37, 38, 39]. Up to now, numerous theoretical and experimental researches have been proposed, such like the cavity optomechanics-based ultralow-threshold phonon lasers [33], the  $\mathcal{PT}$ -symmetric phonon laser with balanced gain and loss [34], the nonreciprocal phonon lasing in a coupled cavity system composed of an optomechanical resonator and a spinning resonator [35], the phonon laser operating at an exceptional point [40], the scheme of amplifying phonon laser by using phonon stimulated emission coherence [41], the phonon-stimulated emission in cryogenic ionic compounds [42, 43], semiconductor superlattices [44] and so on [45, 46, 47, 48]. In addition, phonon lasers have also attracted extensive interest in medical imaging and high-precision measurement equipment.

In this work, we study a cavity magnomechanical system,

\*Corresponding author

Email address: lichong@dlut.edu.com (Chong Li)

which consist of a microwave cavity, a YIG sphere and the uniform external bias magnetic field  $H$  (vertical direction). The uniform magnon mode resonates in the YIG sphere at frequency  $\omega_m = \gamma_g H$  (where  $\gamma_g$  is gyromagnetic ratio). The magnetostrictive (radiation pressure like) interaction mediates the coupling between magnons and phonons. The photons and magnons are coupled via magnetic dipole interaction. It is worth noting that, unlike optical pump in the traditional cavity optomechanical system, we introduce magnetic driving field to realize phonon laser. Furthermore, the magnomechanical interaction which is quite weak in experiment can be enhanced by the gain of magnon mode. We found that unlike the phonon laser in optomechanical system, the production of laser can be well modulated by adjusting the applied magnetic field  $H$ , which provides an additional degree of freedom to control phonon laser action. It is worth mentioning that the applied magnetic field  $H$ , the drive magnetic field, and the magnetic field of the cavity mode are mutually perpendicular at the site of the YIG sphere. So we can adjust only one of them without worrying about the impact on the rest. Finally, we can make our system reach the threshold condition by enhancing drive magnetic field. And the threshold power required can be below  $10\mu\text{W}$  within the experimental allowable range of parameters. According to the recent work, we can find that the threshold power in cavity optomechanical system is generally about  $7\mu\text{W}$  [33, 34, 35]. From the point of threshold power, phonon laser has potential application value in cavity magnomechanical systems.

The structure of the paper is as follows. In Sec. II, we establish physical model and utilize the Heisenberg-Langevin equations of motion to calculate the mechanical gain of phonon laser. In Sec. III, we show the relationship between the distribution of steady-state magnon number and external bias magnetic field  $H$ , and the enhancement of steady-state magnon number by drive magnetic field. In sec. IV, the magnetic field-based control of phonon laser action is illustrated. Finally, we make a conclusion based on the result obtained in sec. V.

## 2. Model and dynamical equations

We consider a hybrid cavity magnomechanical system, which consists a microwave cavity and a small sphere (a highly polished single-crystal YIG sphere of diameter  $1\text{mm}$  is used in [21]), there are three modes in this system: cavity photon mode, magnon mode and phonon mode. As shown in Fig. 1, the YIG sphere is placed near the maximum microwave magnetic field of the cavity mode, and an uniform external bias magnetic field  $H$  is applied along the  $z$  direction to bias the YIG sphere simultaneously, which establish the magnon-photon coupling [21, 20]. The magnons in this system can be tuned by an external magnetic field and the magnon-photon coupling can be tuned by moving the YIG sphere inside the cavity. In addition, the magnetic field  $H$  is created by a high precision tunable electromagnet, and the adjusting range of bias magnetic field  $H$  is between 0 and  $1\text{T}$  [21]. The coupling between magnons and phonons is generated by magnetostrictive interaction (the derivation of the relevant Hamiltonian can be found in [19], and

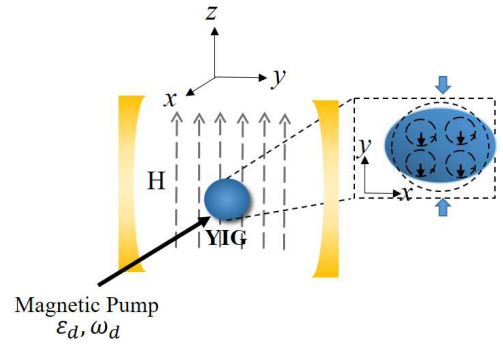


**Fig. 1:** (1)Schematic illustration of the system, a YIG sphere is placed in the maximum magnetic field of a microwave cavity mode. And an uniform external bias magnetic field  $H$  is applied along the  $z$ -direction to bias the YIG sphere. The enlarged YIG sphere on the right illustrates how the dynamic magnetization of magnon (vertical black arrows) causes the deformation (compression along the  $y$ -direction) of the YIG sphere (and vice versa), which rotates at the magnon frequency. Furthermore, a microwave source is used to drive the magnon mode. It's important to note that the bias magnetic field (z direction), the drive magnetic field (y direction), and the magnetic field (x direction) of the cavity mode are mutually perpendicular at the site of the YIG sphere.(2)The equivalent coupled-harmonic-resonator model. (3)Energy levels forming the three-level configuration, denotes the number state with

based on the parameters we choose, the unwanted nonlinear effects due to the Kerr nonlinear term in the Hamiltonian can be neglected [53]). Beause of the varying magnetization induced by the magnon excitation inside the YIG sphere, the sphere produce micro deformation and it can be used as an excellent mechanical resonator. Based on it, we have the vibrational modes (phonons) of the sphere. Here, a microwave source is used to directly drive the magnon mode and it can also enhance the magnomechanical coupling [21, 18]. And we make the bias magnetic field (z-direction), the drive magnetic field (y-direction), and the magnetic field (x-direction) of the cavity mode perpendicular to each other. We concurrently assume that the size of the sphere is so smaller than the wavelength that the interaction between cavity microwave photons and phonons due to the effect of radiation pressure can be neglected. The total Hamiltonian of the hybrid system reads ( $\hbar = 1$ )

$$\begin{aligned} H_{total} &= H_0 + H_{int} + H_d, \\ H_0 &= \omega_a a^\dagger a + \omega_m m^\dagger m + \omega_b b^\dagger b, \\ H_{int} &= g_{ma}(a^\dagger m + m^\dagger a) - g_{mb} m^\dagger m(b + b^\dagger), \\ H_d &= i(\epsilon_d m^\dagger e^{-i\omega_d t} - \epsilon_d^* m e^{i\omega_d t}), \end{aligned} \quad (1)$$

where  $H_0$  is the free Hamiltonian, the first and second terms denote the cavity photon mode and magnon mode, respectively. The third term describes the mechanical mode.  $\omega_a$ ,  $\omega_m$  and  $\omega_b$  denote the resonance frequency of the cavity, magnon, and mechanical mode. Here,  $\omega_m$  is the frequency the Kittel mode (i.e., the ferromagnetic resonance mode) [52]. A uniform magnon mode resonates in the YIG sphere at frequency  $\omega_m = \gamma_g H$ , where  $\gamma_g$  is gyromagnetic ratio and  $\gamma_g/2\pi = 28\text{GHz}/T$ . The annihilation (creation) operators of these modes are  $a(a^\dagger)$ ,  $m(m^\dagger)$  and  $b^\dagger(b)$ , respectively.  $H_{int}$  is the interaction Hamiltonian.

nian of system, the first term of  $H_{int}$  is the coupling between the cavity and magnon mode, the second term represents phonon-magnon interaction.  $g_{ma}$  and  $g_{mb}$  are the coupling rates of the magnon-cavity interaction and the magnon-phonon interaction, respectively. The experimental results show that the coupling strength  $g_{ma}$  can reach strong coupling region. Specifically,  $g_{ma}$  can be larger than the dissipation rates of the cavity and magnon modes ( $g_{ma} > \kappa_a, \kappa_m$ ) [28, 29]. And we can tune  $g_{ma}$  by adjusting the direction of bias field or the position of the YIG sphere inside the cavity. Nevertheless, the single magnon-phonon coupling strength  $g_{mb}$  is very weak in the experiment [19]. And the magnetostrictive coupling strength is determined by the mode overlap between the uniform magnon mode and the phonon modes. Finally,  $H_d$  is the Hamiltonian which describes the external driving of the magnon mode, as shown in [21], J. Q. You *et al* designed an experimental setup, the YIG sphere can be directly driven by a superconducting microwave line which is connected to the external port of the cavity. Rabi frequency  $\varepsilon_d = \frac{\sqrt{5}}{4} \gamma_g \sqrt{M} B_0$  (under the assumption of the low-lying excitations) stands for the coupling strength of the drive magnetic field [18], the amplitude and frequency are  $B_0$  and  $\omega_d$  respectively, the total number of spins  $M = \rho V$ , where  $V$  is the volume of the sphere. Furthermore,  $\rho = 4.22 \times 10^{27} m^{-3}$ , which is the spin density of the YIG sphere.

Then we make a frame rotating at the drive frequency  $\omega_d$  and under the rotating-wave approximation, the total Hamiltonian of the system can be rewritten as

$$\begin{aligned} H_{total} = & -\Delta_a a^\dagger a - \Delta_m m^\dagger m + \omega_b b^\dagger b + \\ & g_{ma}(a^\dagger m + m^\dagger a) - g_{mb} m^\dagger m(b + b^\dagger) \\ & + i(\varepsilon_d m^\dagger - \varepsilon_d^* m), \end{aligned} \quad (2)$$

where  $\Delta_a = \omega_d - \omega_a$  is the detuning between the driving field and cavity mode,  $\Delta_m = \omega_d - \omega_m$  denotes the detuning between the driving field and resonance frequency of cavity mode. The Heisenberg-Langevin equations of the system are given by

$$\begin{aligned} \dot{a} &= (i\Delta_a - \kappa_a)a - ig_{ma}m - \sqrt{2\kappa_a}a_{int}, \\ \dot{m} &= (i\Delta_m - \kappa_m)m - ig_{ma}a + ig_{mb}m(b + b^\dagger) \\ &+ \varepsilon_d - \sqrt{2\kappa_m}m_{int}, \\ \dot{b} &= (-i\omega_b - \gamma_b)b + ig_{mb}m^\dagger m - \xi_{no}, \end{aligned} \quad (3)$$

where  $\gamma_b$  is the mechanical decay rate,  $a_{int}, m_{int}$  and  $\xi_{no}$  are input noise operators of cavity, magnon and mechanical modes respectively.  $\kappa_m$  and  $\kappa_a$  are the losses of magnon mode and microwave cavity mode. Like the computation process of phonon laser [33, 35], for a strong pump field, the mean response of system without including quantum fluctuation is only interested. Therefore the semi-classical Langevin equations of motion are used. In other words, we can rewritten all operators as their respective expectation values, such as  $a = \langle a(t) \rangle$ . And with the mean field approximation  $\langle AB \rangle = \langle A \rangle \langle B \rangle$ , we have following dynamics equations

$$\begin{aligned} \dot{a} &= (i\Delta_a - \kappa_a)a - ig_{ma}m, \\ \dot{m} &= (i\Delta_m - \kappa_m)m - ig_{ma}a \\ &+ ig_{mb}m(b + b^\dagger) + \varepsilon_d, \\ \dot{b} &= (-i\omega_b - \gamma_b)b + ig_{mb}|m|^2, \end{aligned} \quad (4)$$

Assuming that the magnon mode is strongly driven, it leads to the existence of steady-state solutions of the system. From recent experiments using strong driving fields, we can only consider the mean-number behaviors without considering the quantum noise [33]. By setting the left-hand side of Eq.(4) equal to zero, the steady-state mean values of the system read

$$\begin{aligned} a_s &= \frac{g_{ma} \cdot m_s}{\Delta_a - i\kappa_a}, \\ m_s &= \frac{\varepsilon_d}{(\kappa_m - \frac{g_{ma}^2 \Delta_a}{\Delta_a^2 - \kappa_a^2}) - i[\Delta_m + g_{mb}(b_s + b_s^*) + \frac{g_{ma}^2 \kappa_a}{\Delta_a^2 - \kappa_a^2}]}, \\ b_s &= \frac{g_{mb} |m_s|^2}{\omega_b - i\gamma_b}, \end{aligned} \quad (5)$$

Here, according to the feasible experimental parameters ( $g_{mb} < 1\text{Hz}$ ),  $g_{mb}(b_s + b_s^*) \ll \Delta_m$ , under this condition, we approximately have  $\Delta_m + g_{mb}(b_s + b_s^*) \sim \Delta_m$ . In close analogy to an optical laser, a coherent emission of phonons can be achieved with two coupled whispering-gallery-mode microtoroid resonators via inversion of the two optical supermodes. This leads to phenomenon of phonon laser at the breathing mode, with the threshold power  $P_{th} \sim 7\mu\text{W}$  [33, 50]. Similarly, our system also has two supermodes corresponding to the ground and excited state of the two-level atomic system respectively. And mechanical mode (phonon) can realize energy level transition between levels, the stimulated emission of phonon can be generated by virtue of magnetic pumping of the upper level, then leading to the appearance of coherent phonon lasing. Therefore we introduce supermode operators  $\mathfrak{R}_\pm = (a \pm m^\dagger)/\sqrt{2}$  to rewrite the Hamiltonian  $H_0$  and  $H_d$  of the system, i.e.,

$$\begin{aligned} H_{0,sm} &= \omega_+ \mathfrak{R}_+^\dagger \mathfrak{R}_+ + \omega_- \mathfrak{R}_-^\dagger \mathfrak{R}_- + \omega_b b^\dagger b, \\ H_{d,sm} &= i/\sqrt{2} [\varepsilon_d (\mathfrak{R}_+^\dagger + \mathfrak{R}_-^\dagger) - \varepsilon_d^* (\mathfrak{R}_+ + \mathfrak{R}_-)], \end{aligned} \quad (6)$$

where the supermode frequencies  $\omega_\pm = -\frac{\Delta}{2} \pm g_{ma}$ .  $H_{int}$  in Eq.(1) can be tranformed to

$$H_{int} = -\frac{g_{mb}}{2} [(n_+ + n_-) + (\mathfrak{R}_+^\dagger \mathfrak{R}_- + \mathfrak{R}_+ \mathfrak{R}_-^\dagger)](b + b^\dagger), \quad (7)$$

with  $n_+ = \mathfrak{R}_+^\dagger \mathfrak{R}_+$  and  $n_- = \mathfrak{R}_-^\dagger \mathfrak{R}_-$ . In the frame rotating with respect to  $H_{0,sm}$  and applying the rotating-wave approximation,  $H_{int}$  is rewritten as

$$H_{int,sm} = -\frac{g_{mb}}{2} (p^\dagger b + pb^\dagger), \quad (8)$$

where  $\hat{p} = \mathfrak{R}_+ \mathfrak{R}_\dagger$  is the ladder operator. Eq.(8) represents the

absorption and emission of phonons (as in the conventional hybrid optomechanical systems). In general, The introduction of supermode operators  $\mathfrak{R}_{\pm}$  means that the magnon mode and the optical mode have the same resonant frequency. After changing the Hamiltonian into the supermode picture, the equations of motion read

$$\begin{aligned}\dot{\mathfrak{R}}_+ &= -(i\omega_+ + \gamma)\mathfrak{R}_+ + \frac{i}{2}g_{mb}b\mathfrak{R}_- + \frac{\varepsilon_d}{\sqrt{2}}, \\ \dot{\mathfrak{R}}_- &= -(i\omega_- + \gamma)\mathfrak{R}_- + \frac{i}{2}g_{mb}b^\dagger\mathfrak{R}_+ + \frac{\varepsilon_d}{\sqrt{2}}, \\ \dot{b} &= -(i\omega_b + \gamma_b)b + \frac{i}{2}g_{mb}p, \\ \dot{p} &= -2(\gamma + ig_{ma})p - \frac{i}{2}g_{mb}b\Delta n + \frac{1}{\sqrt{2}}(\varepsilon_d\mathfrak{R}_-^\dagger + \varepsilon_d^*\mathfrak{R}_+),\end{aligned}\quad (9)$$

where  $\gamma = (\gamma_a + \gamma_m)/2$ , and  $\Delta n = n_+ - n_-$  is inversion operator. Then we set the left-hand side of Eq.(9) equal to zero, the zero-order steady states of the system are given by

$$\begin{aligned}\mathfrak{R}_{+,s} &= \frac{\sqrt{2}\varepsilon_d[2r + i(2\omega_- + bg_{mb})]}{4(\gamma^2 + g_{ma}^2) - \Delta^2 + g_{mb}^2b^\dagger b - 4i\gamma\Delta}, \\ \mathfrak{R}_{-,s} &= \frac{\sqrt{2}\varepsilon_d[2r + i(2\omega_+ + b^\dagger g_{mb})]}{4(\gamma^2 + g_{ma}^2) - \Delta^2 + g_{mb}^2b^\dagger b - 4i\gamma\Delta}, \\ p &= \frac{\sqrt{2}(\varepsilon_d\hat{a}_-^\dagger + \varepsilon_d^*a_+) - ig_{mb}b\Delta n}{4\gamma + i(4g_{ma} - 2\omega_b)},\end{aligned}\quad (10)$$

where  $\Delta = \Delta_m + \Delta_a$ , then Eq.(10) is substituted into the dynamical equation of  $b$  in Eq.(9), the result can be obtained

$$\dot{b} = \Delta_b b + \chi, \quad (11)$$

with

$$\begin{aligned}\Delta_b &= -i\omega'_b - G - \gamma_b, \\ G &= g_{mb}^2\gamma\left[\frac{\Delta n}{8\gamma^2 + 2\eta^2} + \beta\right], \\ \beta &\simeq \frac{|\varepsilon_d|^2\eta\Delta}{4(\gamma^2 + g_{ma}^2 - \frac{\Delta^2}{4} + \Delta^2\gamma^2)(\eta + 4\gamma^2)},\end{aligned}\quad (12)$$

where  $\eta = 2g_{ma} - \omega_b$ , and the approximation is due to the parameters we have chosen ( $g_{mb} \ll \Delta$ ). Then the inversion operator can be express as

$$\Delta n \simeq \frac{2g_{ma}|\varepsilon_d|^2}{(\gamma^2 + g_{ma}^2 - \frac{\Delta^2}{4})^2 + \gamma^2\Delta^2}. \quad (13)$$

Because this paper mainly studies the phonon laser generated by the system, we are only interested in  $G$ , which indicate the mechanical gain of system. Therefore, only the specific expression of  $G$  is given. The non-negative mechanical gain  $G$  decreases the effective damping rate of the mechanical mode  $\gamma_{eff} = \gamma_b - G$ , that leads to the instabilities of the mechanical oscillator at  $\gamma_{eff} < 0$ . This problem has been analyzed and discussed in [33, 35, 49] from both theoretical and experimental

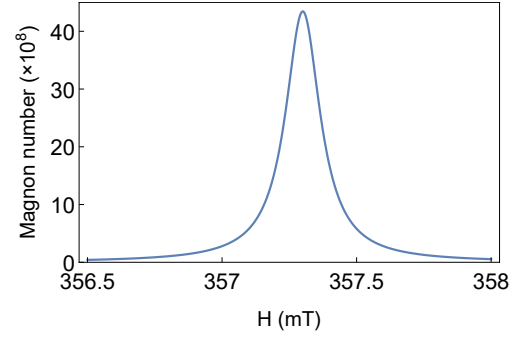


**Fig. 2:** The distribution of steady-state magnon number  $|m_s|^2$  versus the external magnetic field  $H$ . The parameters we used are  $\kappa_m = \kappa_a = 4\text{MHz}$  and  $\varepsilon_d = 1.45 \times 10^{11}\text{Hz}$  ( $B_0 = 0.05\mu\text{T}$ ).

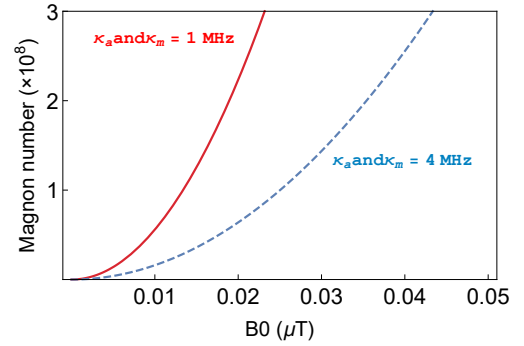


**Fig. 3:** The distribution of steady-state magnon number  $|m_s|^2$  versus the drive magnetic field  $B_0$  under  $\kappa_m = \kappa_a = 1\text{MHz}$  (red solid line) and  $\kappa_m = \kappa_a = 4\text{MHz}$  (blue dashed line).. The parameter we used is  $\Delta_m/2\pi = 8\text{MHz}$ .

perspectives.

### 3. The distribution of steady-state magnon number

Here, we give the specific values of the parameters used in this paper and all parameters used are experimentally feasible parameters [19].  $\omega_a/2\pi = \omega_m/2\pi = 10.1\text{GHz}$ ,  $\omega_b/2\pi = 12\text{MHz}$ ,  $g_{ma}/2\pi = 6\text{MHz}$ ,  $g_{mb}/2\pi = 0.1\text{Hz}$ ,  $\Delta_a/2\pi = 8\text{MHz}$ , and the loss of mechanical modes  $\gamma_b/2\pi = 100\text{Hz}$ . The drive power  $P = (B_0^2/2\mu_0)Ac$  [18], where  $B_0^2/2\mu_0$  is time average of energy per unit volume,  $c$  is the speed of an electromagnetic wave propagating through the vacuum and  $A$  is the maximum cross-sectional area of YIG sphere.

In Fig. 2, we exhibit the effect of external bias magnetic field  $H$  on the steady-state populations of magnons  $|m_s|^2$ . Similar to the study of phonon lasers in cavity optomechanical systems, we show the behavior of magnon number which are interacting with phonons. It is seen that there is a window between about  $357\text{mT}$  and  $357.5\text{mT}$  for  $H$ , and in this window, the system generates a large number of magnons (The eighth order of magnitude of 10). That change in the number of magnons then modifies the magnetostrictive interaction. It is worth mentioning that we set the amplitude of drive magnetic field  $B_0 = 0.05\text{mT}$ , corresponding to the drive power  $P = 5.86\mu\text{W}$ , and this power is much less than the driving power used in [18, 21, 20] (The power they use is in the order of  $\text{mW}$ ).

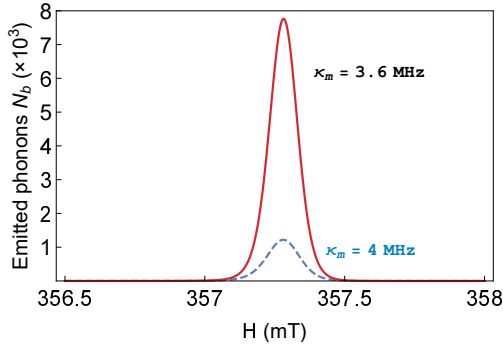


**Fig. 4:** The stimulated emitted phonon number  $n_b$  versus the external bias magnetic field  $H$  under  $\kappa_m = 3.6\text{MHz}$  (red solid line) and  $\kappa_m = 4\text{MHz}$  (blue dashed line). The parameter we used is  $\varepsilon_d = 1.45 \times 10^{11}\text{Hz}$  ( $B_0 = 2\mu\text{T}$ ,  $P = 23\mu\text{W}$ ) and  $\kappa_a = 3\text{MHz}$ .

Fig. 3 shows the distribution of steady-state magnon number  $|m_s|^2$  versus the drive magnetic field  $B_0$ . The number of magnons increases exponentially with the increase of  $B_0$ . Note that the order of drive power  $P$  is  $\mu\text{W}$ , and its corresponding  $B_0$  is very weak relative to the external magnetic field  $H$ . In addition, the results under different losses of magnon mode and microwave cavity mode are also given. It can be seen that the losses is small,  $|m_s|^2$  increases faster, and they have a significant impact.

#### 4. Magnetic field-based control of phonon laser action

In order to explore the relationship between the generation of phonon laser and magnetic field (including the external bias magnetic field  $H$  and the drive magnetic field  $B_0$ ), we investigate the phonon number as a function of  $H$  and  $B_0$ . First, the mechanical gain  $G$  has been given in Eq.(12), thus the stimulated emitted phonon number can be calculated [34, 35], i.e.,

$$n_b = \exp[2(G - \gamma_b)/\gamma_b], \quad (14)$$

then from the above expression, we can get the threshold condition of phonon laser. When  $n_b = 1$ , we have

$$B_{0,th} = \frac{8\sqrt{\frac{2}{5}}\gamma_b\Gamma}{g_{mb}\sqrt{g_{ma}M\gamma\Delta}}, \quad (15)$$

where  $\Gamma = g_{ma}^4 + 2g_{ma}^2(\gamma^2 - \frac{\Delta^2}{4}) + (\gamma^2 + \frac{\Delta^2}{4})^2$ . Here,  $B_{0,th}$  is the driving magnetic field required to achieve the threshold condition of the phonon laser in our system. Finally, according to the expression given earlier  $P = (B_0^2/2\mu_0)Ac$ , the threshold power is defined as

$$P_{th} = \frac{64}{5} \frac{Ac\gamma_b\Gamma}{g_{mb}^2 g_{ma} M \gamma \mu_0 \Delta}, \quad (16)$$

In Fig. 4,  $n_b$  is plotted as a function of the external bias magnetic field  $H$ . There is an obvious window between  $H \approx 357\text{mT} - 357.5\text{mT}$  that generates a large number of the stimulated emitted phonon. This behavior is consistent with previous

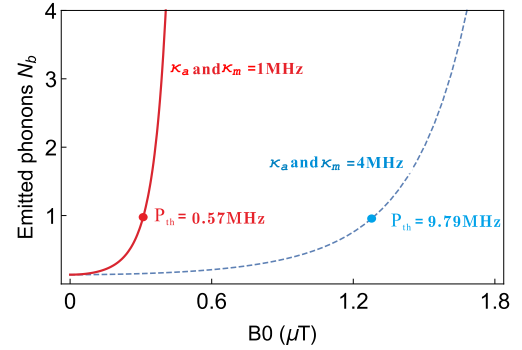


**Fig. 5:** The stimulated emitted phonon number  $n_b$  versus the drive magnetic field  $B_0$  under  $\kappa_m = \kappa_a = 1\text{MHz}$  (red solid line,  $P_{th} = 0.57\mu\text{W}$ ) and  $\kappa_m = \kappa_a = 4\text{MHz}$  (blue dashed line,  $P_{th} = 9.79\mu\text{W}$ ). The other parameter we used is  $\Delta_m/2\pi = 8\text{MHz}$ .

effect on the number of magnons. And we find that the distribution of the stimulated emitted phonon number has a Lorentzian-like shape dependence on the applied magnetic field, which presents an additional degree of freedom to control phonon laser. And that phenomenon similar to a switch of a phonon laser can be obtained by adjusting  $H$  without changing other parameters. Especially, the widths of the windows almost keep unchanged with the loss of magnon mode  $\kappa_m$ . Moreover, it can be seen that the number of phonons increases with decreasing  $\kappa_m$ . In Fig. 5,  $n_b$  is plotted as a function of the drive magnetic field  $B_0$ , the stimulated emitted phonon number is enhanced by input driving magnetic field. The losses of magnon mode and cavity mode both have significant impacts on the threshold power  $P_{th}$ . For  $\kappa_m = \kappa_a = 1\text{MHz}$  and  $\kappa_m = \kappa_a = 4\text{MHz}$ , we have  $P_{th} \sim 0.57\mu\text{W}$  and  $P_{th} \sim 9.79\mu\text{W}$ , respectively. It is worth mentioning that  $P_{th}$  is calculated in the range of parameters that can be achieved by experiments, and it is not much different from the  $P_{th}$  obtained in the cavity optomechanics system, and the threshold power in cavity optomechanical system is generally about  $7\mu\text{W}$  in [33, 34, 35, 51].

#### 5. Conclusion

In summary, we have investigated theoretically phonon laser in a hybrid cavity magnomechanical system, which use magnetostrictive force (radiation pressure like) to achieve interaction between magnon mode and mechanical mode. Different from the phonon laser action previously discussed, our results have shown that by adjusting the the external bias magnetic field  $H$ , a window which generates a large number of phonons can be obtained. And the width of this window is about  $0.5\text{mT}$ . Compared with the conventional phonon laser work [33, 34, 35], our scheme provides an additional degree of freedom to control phonon laser action. In addition, we use a novel drive magnetic field, which can be realized by directly driving the YIG sphere with a microwave source. By increasing the drive magnetic field  $B_0$ , the system can reach the threshold power and produce phonon laser. With the experimentally feasible parameters, threshold power  $P_{th}$  in our system is close to the threshold power of phonon laser in optomechanical systems which are

mature in theory and experiment. We believe that the proposed scheme provides a new idea for magnetic-optics field. Finally, we hope that the phonon laser in the hybrid cavity magnomechanical system will be accessible in the near future.

## 6. acknowledgments

This work was supported by the National Natural Science Foundation of China, under Grant No. 11574041 and No. 11475037.

## 7. References

### References

- [1] M. Aspelmeyer, T. J. Kippenberg, and F. Marquardt, "Cavity optomechanics," *Rev. Mod. Phys.* **86**, 1391 (2014).
- [2] M. W. Li, H. P. Pernice, C. Xiong, and H. X. Tang, "Harnessing optical forces in integrated photonic circuits," *Nature* **456**, 480 (2008).
- [3] A. H. Safavi-Naeini, T. P. Mayer Alegre, J. Chan, M. Eichenfield, and O. Painter, "Electromagnetically induced transparency and slow light with optomechanics," *Nature* **472**, 69 (2011).
- [4] J. G. Huang, Y. Li, L. K. Chin, H. Cai, Y. D. Gu, M. F. Karim, J. H. Wu, T. N. Chen, Z. C. Yang, Y. L. Hao, C. W. Qiu, and A. Q. Liu, "A dissipative self-sustained optomechanical resonator on a silicon chip," *Appl. Phys. Lett.* **112**, 051104 (2018).
- [5] J. Vovrosh, M. Rashid, D. Hempston, J. Bateman, M. Paternostro, and H. Ulbricht, "Parametric feedback cooling of levitated optomechanics in a parabolic mirror trap," *J. Opt. Soc. Am. B* **34**, 1421-1428 (2017).
- [6] X. Y. Zhang, Y. H. Zhou, Y. Q. Guo, and X. X. Yi, "Double optomechanically induced transparency and absorption in parity-time-symmetric optomechanical systems," *Phys. Rev. A* **98**, 033832 (2018).
- [7] Q. Wu, J. Q. Zhang, J. H. Wu, M. Feng, and Z. M. Zhang, "Tunable multi-channel inverse optomechanically induced transparency and its applications," *Opt. Express* **23**, 18534 (2015).
- [8] B. Xiong, Li. X, S. L. Chao, and L. Zhou, "Optomechanical quadrature squeezing in the non-Markovian regime," *Opt. Lett.* **43**, 6053-6056 (2018).
- [9] W. Li, C. Li, and H. Song, "Quantum synchronization in an optomechanical system based on Lyapunov control," *Phys. Rev. E* **93**, 06222 (2016).
- [10] P. Rabl, "Photon blockade effect in optomechanical systems" *Phys. Rev. Lett.* **107**, 063601 (2011).
- [11] G. Heinrich, M. Ludwig, J. Qian, B. Kubala, and F. Marquardt, "Collective dynamics in optomechanical arrays," *Phys. Rev. Lett.* **107**, 043603 (2011).
- [12] T. P. Purdy, P. L. Yu, R. W. Peterson, N. S. Kampel, and C. A. Regal, "Strong optomechanical squeezing of light," *Phys. Rev. X* **3**, 031012 (2013).
- [13] J. Q. Liao, and F. Nori, "Photon blockade in quadratically coupled optomechanical systems," *Phys. Rev. A* **88**, 023853 (2013).
- [14] Y. X. Zeng, T. Gebremariam, M. S. Ding, and C. Li, "Quantum optical diode based on Lyapunov control in a superconducting system" *J. Opt. Soc. Am. B* **35**, 2334 (2018).
- [15] R.W. Andrews, R.W. Peterson, T. P. Purdy, K. Cicak, R.W. Simmonds, C. A. Regal, and K.W. Lehnert, "Bidirectional and efficient conversion between microwave and optical light," *Nat. Phys.* **10**, 321-326 (2014).
- [16] T. Bagci, A. Simonsen, S. Schmid, L. G. Villanueva, E. Zeuthen, J. Appel, J. M. Taylor, A. Soensen, K. Usami, A. Schliesser, and E. S. Polzik, "Optical detection of radio waves through a nanomechanical transducer," *Nature* **507**, 81-85 (2014).
- [17] L. Fan, K. Y. Fong, M. Poot, and H. X. Tang, "Cascaded optical transparency in multimode-cavity optomechanical systems," *Nat. Commun.* **6**, 5850 (2015).
- [18] J. Li, S. Y. Zhu, and G. S. Agarwal, "Magnon-photon-phonon entanglement in cavity magnomechanics". *Phys. Rev. Lett.* **121**, 203601 (2018).
- [19] X. Zhang, C. L. Zou, L. Jiang, and H. X. Tang, "Cavity magnomechanics," *Sci. Adv.* **2**, e1501286 (2016).
- [20] Y. P. Wang, G. Q. Zhang, D. Zhang, T. F. Li, C. M. Hu, and J. Q. You, "Bistability of Cavity Magnon Polaritons," *Phys. Rev. Lett.* **120**, 057202 (2018).
- [21] Y. P. Wang, G. Q. Zhang, D. Zhang, X. Q. Luo, W. Xiong, S. P. Wang, T. F. Li, C. M. Hu, and J. Q. You, "Magnon Kerr effect in a strongly coupled cavity-magnon system," *Phys. Rev. B* **94**, 224410 (2016).
- [22] Z. X. Liu, B. Wang, H. Xiong, and Y. Wu, "Magnon-induced high-order sideband generation," *Opt. Lett.* **43**, 3698 (2018).
- [23] X. R. Xiong, Y. P. Gao, X. F. Liu, C. Cao, T. J. Wang, and C. Wang, "The analysis of high-order sideband signals in optomechanical system," *Sci. China. Phys. Mech.* **61**, 90322 (2018)
- [24] B. Wang, Z. X. Liu, C. Kong, H. Xiong, and Y. Wu, "Magnon-induced transparency and amplification in PTsymmetric cavity-magnon system," *Opt. Express* **26**, 20248-20257 (2018).
- [25] L. M. Woods, "Magnon-phonon effects in ferromagnetic manganites," *Phys. Rev. B* **65**, 014409 (2001).
- [26] A. M. Kalashnikova, A. V. Kimel, R. V. Pisarev, V. N. Gridnev, P. A. Usachev, A. Kirilyuk, and T. Rasing, "Impulsive excitation of coherent magnons and phonons by subpicosecond laser pulses in the weak ferromagnet FeBO<sub>3</sub>," *Phys. Rev. B* **78**, 104301 (2008).
- [27] Y. P. Gao, C. Cao, T. J. Wang, Y. Zhang, and C. Wang, "Cavity-mediated coupling of phonons and magnons," *Phys. Rev. A* **96**, 023826 (2017).
- [28] X. Zhang, C. L. Zou, L. Jiang, and H. X. Tang, "Strongly coupled magnons and cavity microwave photons," *Phys. Rev. Lett.* **113**, 156401 (2014).
- [29] L. Bai, M. Harder, Y. P. Chen, X. Fan, J. Q. Xiao, and C.-M. Hu, "Spin Pumping in Electro-dynamically Coupled Magnon-Photon Systems," *Phys. Rev. Lett.* **114**, 227201 (2015).
- [30] M. Goryachev, W. G. Farr, D. L. Creedon, Y. Fan, and M. E. Tobar, "High-cooperativity cavity QED with magnons at microwave frequencies," *Phys. Rev. Applied* **2**, 054002 (2014).
- [31] R. Bonifacio, and L. De. Salvo, "Collective atomic recoil laser (CARL) optical gain without inversion by collective atomic recoil and self-bunching of two-level atoms," *Nucl. Instrum. Method Phys. Res. Sect. A* **341**, 360 (1994).
- [32] D. J. Gauthier, Q. Wu, S. E. Morin, and T. W. Mossberg, "Realization of a continuous-wave, two-photon optical laser," *Phys. Rev. Lett.* **68**, 464 (1992).
- [33] I. S. Grudinin, H. Lee, O. Painter, and K. J. Vahala, "Phonon laser action in a tunable two-level system," *Phys. Rev. Lett.* **104**, 083901 (2010).
- [34] H. Jing, S. K. ozdemir, X. Y. Lü, J. Zhang, L. Yang, and F. Nori, "PT-Symmetric Phonon Laser," *Phys. Rev. Lett.* **113**, 053604 (2014).
- [35] Y. Jiang, S. Maayani, T. Carmon, F. Nori, and H. Jing, "Nonreciprocal Phonon Laser Phys," *Rev. Applied* **10**, 064037 (2018).
- [36] J. Chen, and J. B. Khurgin, "Feasibility analysis of phonon lasers," *IEEE. J. Quantum. Elect.* **39**, 600 (2003).
- [37] S. Wallentowitz, W. Vogel, I. Siemers, and P. E. Toschek, "Vibrational amplification by stimulated emission of radiation," *Phys. Rev. A* **54**, 943 (1996).
- [38] A. Khaetskii, V. N. Golovach, X. Hu, and I. Žutić, "Proposal for a phonon laser utilizing quantum-dot spin states," *Phys. Rev. Lett.* **111**, 186601 (2013).
- [39] J. Kabuss, A. Carmele, T. Brandes, and A. Knorr, "Optically driven quantum dots as source of coherent cavity phonons: a proposal for a phonon laser scheme," *Phys. Rev. Lett.* **109**, 054301 (2012).
- [40] J. Zhang, B. Peng, and L. Yang, "A phonon laser operating at an exceptional point," *Nat. Photonics.* **12**,479 (2018).
- [41] I. Mahboob, K. Nishiguchi, A. Fujiwara, and H. Yamaguchi, "Phonon lasing in an electromechanical resonator," *Phys. Rev. Lett.* **110**, 127202 (2013).
- [42] P. A. Fokker, J. I. Dijkhuis, and H. W. deWijn, "Stimulated emission of phonons in an acoustical cavity," *Phys. Rev. B* **55**, 2925 (1997).
- [43] Bron W E and Grill W "Stimulated phonon emission," *Phys. Rev. Lett.* **40**, 1459 (1978).
- [44] A. J. Kent, R. N. Kini, N. M. Stanton, M. Henini, and T. L. Linnik, "Acoustic phonon emission from a weakly coupled superlattice under vertical electron transport: observation of phonon resonance," *Phys. Rev. Lett.* **96**, 215504 (2006).
- [45] K. Vahala, M. Herrmann, V. Batteiger, G. Saathoff, and T. Udem, "A phonon laser," *Nat. Phys.* **5**, 682 (2009).
- [46] B. He, L. Yang, and M. Xiao, "Dynamical phonon laser in coupled active-

passive microresonators," Phys. Rev. A **94**, 031802 (2016).

[47] M. Herrmann, V. Batteiger, G. Saathoff, T. W. Hsch, and T. Udem, "Injection locking of a trapped-ion phonon laser," Phys. Rev. Lett. **105**, 013004 (2010).

[48] I. Mahboob, K. Nishiguchi, A. Fujiwara, and H. Yamaguchi, "Phonon lasing in an electromechanical resonator," Phys. Rev. Lett. **110**, 127202 (2013).

[49] J. D. Cohen, S. M. Meenehan, G. S. MacCabe, F. Marsili, M. D. Shaw, and O. Painter, Nature **520**, 522 (2015)

[50] G. Wang, M. Zhao, Y. Qin, Z. Yin, X. Jiang, and M. Xiao, "Demonstration of an ultra-low-threshold phonon laser with coupled microtoroid resonators in vacuum," Photon. Res. **5**, 73 (2017)

[51] B. Wang, Z. X. Liu, X. Jia, and Y. Wu, "Polarization-based control of phonon laser action in a Parity Time-symmetric optomechanical system," Commun. Phys. **43**, 1 (2018).

[52] C. Kittel, "On the theory of ferromagnetic resonance absorption," Phys. Rev. **73**, 155 (1948)

[53] J. Li, S. Y. Zhu, and G. S. Agarwal, "Squeezed states of magnons and phonons in cavity magnomechanics," Phys. Rev. A **99**, 021801 (2019).